Modeling the bremsstrahlung emission from converters

M. Mirea, O. Bajeat, F. Clapier, M. Hassaine, F. Ibrahim, A.C. Mueller, N. Pauwels, J. Proust, D. Verney, R. Antoni, et al.

MODELING THE BREMSSTRAHLUNG EMISSION FROM CONVERTERS *

M. Mirea[1,2], O. Bajeat[1], F. Clapier[1], M. Hassaine[2,3],
F. Ibrahim[1], A.C. Mueller[1], N. Pauwels[1],
J. Proust[1], D. Verney[1]†, R. Antoni[4], L. Bourgois[4] and S. Kandri-Rody[1,5]

[1]Institut de Physique Nucléaire, 91406 Orsay Cedex, France
[2]Institute of Physics and Nuclear Engineering, P.O. Box MG-6, Bucarest, Romania
[3]Université de Tours, 37200 Tours, France
[4]Commissariat à l'Énergie Atomique Saclay, 91191 Gif sur Yvette, France
[5]Université Chouaib Doukkali, BP 20 El Jadida, Maroc

Abstract

The bremsstrahlung angular and energy theoretical distributions delivered from W and UCx thick converters are reported. This study is focussed on initial kinetic energies of the electron beam included in the range 30–60 MeV, suitable for the production of large radiative yields able to induce the ^{238}U fission. These results offer the possibility to evaluate the required shielding for a neutron rich nuclei source.

INTRODUCTION

Nuclear fission of heavy nuclei is a process which allows the production of neutron rich isotopes. Exploiting this property, a source of nuclei near the stability limit can be conceived. The feasibility study of an exotic nuclei source involving the fission process represents the main objective of the PARRNe (Production d'Atomes Radioactif Riches en Neutrons) R&D project. Two different concepts have been studied to build such a source. The first one, is based on the neutron induced fission of ^{238}U. A high neutron flux can be produced by using the deuteron break–up reaction. Experimental and theoretical results concerning the analysis of this concept are reported by Clapier and al., Rody and al., Mirea and al.[1,2,3]. Secondly, in a competitive manner, it is intended to study the feasibility of an exotic nuclei source by involving the bremsstrahlung induced fission. In a first step, an electron beam of 30-60 MeV is focussed onto a W converter or onto the uranium carbide target (UCx) itself to deliver a bremsstrahlung radiation. In the second step, the gamma rays induce the fission of the ^{238}U. To realize such an experimental combination, accurate knowledge of the bremsstrahlung spectrum is essential. This work is mainly concerned on the bremsstrahlung distributions evaluation in order to serve several purposes: shielding the radiation, estimating the electron energy loss in the converter, or estimating the neutron rich nuclei yields in the target. Since the experimental systematic of bremsstrahlung spectra is not accurate, and the coverage is too sparse, one must rely on the theoretical results. The next section is devoted to this subject.

*submited to RADIATION PROTECTION DOSIMETRY
†Present address: Grand Accélérateur National d'Ions Lourds, 14021 Caen Cedex, France

THEORETICAL GUIDELINE

In this section, the main steps used to deduce the bremsstrahlung emission from targets are overviewed. The distributions of the electrons inside a target are obtained using single and multiple scattering theories. The differential bremsstrahlung emission is determined by selecting formulas and correction factors that give the best estimate for the cross section. The angular distribution of the gamma rays is finally deduced by applying the folding theorem between the angular electron spread and the differential bremsstrahlung cross section. The slowing down of the electrons is estimated to obtain the mean energy along the range. Integrating the irradiated flux along the electron range, the absorption of the continuous bremsstrahlung in the converter (or in the target) is taken into account. The shape of the converter is considered as cylindrical. Secondary electrons are produced with small kinetic energies which are not sufficient to produce gamma rays soft enough to induce fission, so, this effect is disregarded. To avoid long computational time, the electron energy spread is not included.

Electron distributions

The angular and the projected distributions of the electrons at a depth d inside the target are obtained following the prescriptions of Knop and Paul[4] concerning the valability of the Mott's cross section and the Molière's distributions. Therefore, if the depth where the electron distribution is determined is very small, that means the condition $d << \frac{1}{\sigma N}$ is fulfilled (where σ is the cross section and N the number of atoms per volume unity), we use the Mott cross section:

$$\frac{\mathrm{d}\sigma}{\mathrm{d}\Omega} = \frac{Z^2 r_0^2}{4\sin^4\frac{\theta}{2}} \frac{1}{E^2\left(1-\frac{1}{E^2}\right)} R(E,Z,\theta) r(E,Z,\theta) \tag{1}$$

where $R(E,Z,\theta)$ is the ratio between the cross section at high energy and the Rutherford's classical Coulomb scattering cross section, $r(E,Z,\theta)$ denotes a correction due to the shielding, $r_0 = 2.8 \times 10^{-13}$ cm is the classical electron radius and E is the total energy of the electron in mc^2 units. The ratio $R(E,Z,\theta)$ is calculated with respect to the prescriptions given by McKinley and Feshbach[5] while values for $r(E,Z,\theta)$ are extracted from the literature[6]. Throughout this paper, Z and A denotes the atomic and the mass numbers of the converter. The probability that the electron is not deviated up to the depth d is:

$$P(\theta = 0, d) = 1 - 2\pi N d \int_0^{\pi} \frac{\mathrm{d}\sigma}{\mathrm{d}\Omega} \sin\theta \mathrm{d}\theta \tag{2}$$

In this domain, the differential projected distribution $W(\rho, d, z)$ can be deduced:

$$W(\rho,d,z)\rho\mathrm{d}\rho = 2\pi N \frac{\mathrm{d}\sigma(\theta_\rho)}{\mathrm{d}\Omega} \frac{\cos\theta_\rho}{\rho^2 + (d-z)^2} \mathrm{d}z \tag{3}$$

where

$$\theta_\rho = \arctan\left(\frac{\rho}{d-z}\right) \tag{4}$$

So, $W(\rho, d, z)$ represents the probability that the electron deviates from its original direction (where the cylindrical coordinates $\rho = 0$) to attain the ring surface $\rho\mathrm{d}\rho$ around the initial direction, situated at the depth d due to a scattering along a range $\mathrm{d}z$. Therefore, the probability $W(\theta_0, d)$ to obtain the electron in an angular interval $\mathrm{d}\theta_0$ measured from the entrance side (z=0) of the converter at the depth d becomes:

$$W(\theta_0,d) = 2\pi d^2 \frac{\tan\theta_0}{\cos^2\theta_0} \int_0^d N \frac{\mathrm{d}\sigma\left[\arctan\left(\frac{\rho}{d-x}\right)\right]}{\mathrm{d}\Omega} \frac{\cos\left[\arctan\left(\frac{\rho}{d-x}\right)\right]}{\rho^2 + (d-z)^2} \mathrm{d}z \tag{5}$$

This last relation allows the determination of the lateral distribution of the electrons at different depths in the target.

If the depth d becomes greater or equal to $\frac{1}{\sigma N}$, we used the multiple scattering of Molière[6] In the framework of this theory, the averaged angular distribution of multiple scattering is:

$$F(\theta,d)=\frac{1}{2\pi}\left[2\exp(-\eta^2)+\frac{1}{B}F^1(\eta)+\frac{1}{B^2}F^2(\eta)\right] \tag{6}$$

with $\eta=\theta/(\theta_1\sqrt{B})$ being an reduced angle, $\theta_1=0.3965Z(Z+1)/(mc^2p\beta)\sqrt{\rho d/A}$, ρ is the density, p is momentum in mc unit, mc^2=0.51 MeV, the parameter B is the solution of the equation

$$\ln B-B+\ln\gamma-0.154=0 \tag{7}$$

where $\gamma=8.831\times10^3q(Z+1)Z^{1/3}\rho d/(\beta^2A\Delta)$, $\Delta=1.13+32Z^2/(137\beta)$. Values for the parameters p and β are obtained with the formulas given in the next section. The normalization condition

$$2\pi\int_0^{\pi/2}F(\theta,d)\sin\theta\,\mathrm{d}\theta=1 \tag{8}$$

must be satisfied. This last condition in the small angle approximation reads:

$$2\pi\int_0^{\infty}F(\theta,d)\theta\,\mathrm{d}\theta=1 \tag{9}$$

For multiple scattering, the projected distribution f as function of an angle θ_0 measured from the origin (z=0) is:

$$f(\theta_0,d)=\frac{2}{\sqrt{\pi}}\exp\left[-\left(\frac{\theta_0}{\eta B^{1/2}}\right)^2\right]+\frac{1}{B}f^1\left(\frac{\theta_0}{\eta B^{1/2}}\right)+\frac{1}{B^2}f^2\left(\frac{\theta_0}{\eta B^{1/2}}\right) \tag{10}$$

with the condition

$$\int_0^{\infty}f(\theta_0,d)\mathrm{d}\theta_0=1 \tag{11}$$

Values for F^i and f^i are tabulated in the literature[6].

An interpolation is realized in the plural scattering domain between the expressions deduced for single scattering and multiple scattering.

Bremsstrahlung distributions

The choice of the bremsstrahlung differential cross-section in photon energy and angle formulas as function of the electron energy was guided by the prescriptions given by Koch and Motz[7] and Berger and Seltzer[8]

$$\frac{\mathrm{d}^2\sigma}{\mathrm{d}k\mathrm{d}\Omega}=\begin{cases}\mathcal{A}f_E\frac{\mathrm{d}^2\sigma^{2\mathrm{BN}}}{\mathrm{d}k\mathrm{d}\Omega} & \text{for } E_e<2\text{ MeV}\\ \mathcal{A}\frac{\mathrm{d}^2\sigma^{2\mathrm{BN}}}{\mathrm{d}k\mathrm{d}\Omega} & \text{for } 2\text{ MeV}<E_e<50\text{ MeV and } \gamma\geq15\\ \mathcal{A}\frac{\mathrm{d}^2\sigma^{2\mathrm{BS}}}{\mathrm{d}k\mathrm{d}\Omega} & \text{for } 2\text{ MeV}<E_e<50\text{ MeV and } \gamma<15\\ \frac{\mathrm{d}^2\sigma^{2\mathrm{BN}}}{\mathrm{d}k\mathrm{d}\Omega} & \text{for } 50\text{ MeV}<E_e<100\text{ MeV and } \gamma\geq15\\ \frac{\mathrm{d}^2\sigma^{2\mathrm{CS}}}{\mathrm{d}k\mathrm{d}\Omega} & \text{for } 50\text{ MeV}<E_e<100\text{ MeV and } \gamma<15\end{cases} \tag{12}$$

where E_e is the electron kinetic energy. Here, we used the Born approximation cross section 2BN and 2BS formulas and the relativistic cross section 2CS formulas with Coulomb correction. The 2BS formula is:

$$\frac{\mathrm{d}^2\sigma^{2\mathrm{BS}}}{\mathrm{d}k\mathrm{d}\Omega}=\frac{4Z^2r_0^2}{137k}\frac{yE}{2\pi\sin\theta}\left\{\frac{16y^2E'}{(y^2+1)^4E}-\frac{(E+E')^2}{(y^2+1)^2E^2}+\left[\frac{E^2+E'^2}{(y^2+1)^2E^2}-\frac{4y^2E'}{(y^2+1)^4E}\right]\ln M(y)\right\} \tag{13}$$

where,

$$y = E\theta \tag{14}$$

$$\frac{1}{M(y)} = \left(\frac{k}{2EE'}\right)^2 + \left[\frac{Z^{1/3}}{111(y^2+1)}\right]^2 \tag{15}$$

The 2BN formula is

$$\begin{array}{c}\frac{\mathrm{d}^2\sigma^{2\mathrm{BN}}}{\mathrm{d}k\mathrm{d}\Omega} = \frac{Z^2 r_0^2}{8\pi 137}\frac{1}{k}\frac{p'}{p}\left\{\frac{8\sin^2\theta(2E^2+1)}{p^2\Delta^4} - \frac{2(5E^2+2EE'+3)}{p^2\Delta^2} - \frac{2(p^2-k^2)}{Q^2\Delta^2} + \frac{4E'}{p^2\Delta} + \right. \\ \left.\frac{L}{pp'}\left[\frac{4E\sin^2\theta(3k-p^2E')}{p^2\Delta^4} + \frac{4E^2(E^2+E'^2)}{p^2\Delta^2} + \frac{2-2(7E^2-3EE'+E'^2)}{p^2\Delta^2} + \frac{2k(E^2+EE'-1)}{p^2\Delta}\right] - \right. \\ \left.\left(\frac{4\epsilon}{p'\Delta}\right) + \left(\frac{\epsilon^Q}{p'Q}\right)\left[\frac{4}{\Delta^2} - \frac{6k}{\Delta} - \frac{2k(p^2-k^2)}{Q^2\Delta}\right]\right\}\end{array} \tag{16}$$

where

$$L = \ln\left[\frac{EE' - 1 + pp'}{EE' - 1 - pp'}\right] \tag{17}$$

$$\Delta = E - p\cos\theta \tag{18}$$

$$\epsilon = \ln\left(\frac{E' + p'}{E' - p'}\right) \tag{19}$$

$$\epsilon^Q = \ln\left(\frac{Q + p'}{Q - p'}\right) \tag{20}$$

$$Q^2 = p^2 + k^2 - 2pk\cos(\theta) \tag{21}$$

The 2CS formula is

$$\begin{array}{c}\frac{\mathrm{d}^2\sigma^{2\mathrm{CS}}}{\mathrm{d}k\mathrm{d}\Omega} = \frac{2Z^2 r_0^2}{137}\frac{1}{k}\frac{2pu}{(1+u^2)}\frac{1}{2\pi\sin\theta}\frac{1}{E^2}\times \\ \left\{(E^2+E'^2)(3+2\Gamma) - 2EE'(1+4u^2\epsilon^2\Gamma)\right\}\end{array} \tag{22}$$

where

$$\epsilon = \frac{1}{1+u^2} \tag{23}$$

$$u = p\theta \tag{24}$$

$$\Gamma = \ln\left(\frac{111Z^{-1/3}}{\epsilon}\right) - 2 - f(Z) \tag{25}$$

$$f(Z) = \left\{\begin{array}{ll} 1.2021(Z/137)^2 & \text{for low } Z \\ 0.925(Z/137)^2 & \text{for high } Z\end{array}\right. \tag{26}$$

In the previous relations, E is the total electron energy in mc^2 units, $E' = E - k$ is the final energy of the electron after the emission of a quanta of energy k, p and p' are the initial and final momentum of the electron in mc units:

$$\begin{array}{c} p = \sqrt{(E-1)(E+1)} \\ p' = \sqrt{(E'-1)(E'+1)} \\ \beta = \frac{p}{E}\end{array} \tag{27}$$

Also, $\mathcal{A}$ represents a corrective factor for the Born approximation obtained by interpolating the data of Koch and Motz[7], f_E is the Elwert factor restricted to nonrelativistic electron energies:

$$f_E = \frac{\beta\{1 - \exp[-2\pi Z/(137\beta)]\}}{\beta'\{1 - \exp[-2\pi Z/(137\beta')]\}} \tag{28}$$

and $\gamma = 100k(EE'Z^{1/3})^{-1}$ is a screening factor.

Folding the electron and gamma distributions

The folding theorem is applied to obtain the angular distribution. As prescribed by Scott[6], the folding theorem for spatial distributions reads:

$$\begin{gathered} F(\theta,\varphi) = F\left(\arctan\sqrt{\tan^2\psi_x+\tan^2\psi_y}, \arctan\frac{\tan\psi_y}{\tan\psi_x}\right) = \\ \int_{-\pi}^{\pi} d\psi_{1x}\int_{-\pi}^{\pi} d\psi_{1y} F_1\left(\arctan\sqrt{\tan^2\psi_{1x}+\tan^2\psi_{1y}}, \arctan\frac{\tan\psi_{1y}}{\tan\psi_{1x}}\right)\times \\ F_2\left[\arctan\sqrt{\tan^2(\psi_x-\psi_{1x})+\tan^2(\psi_y-\psi_{1y})}, \arctan\frac{\tan(\psi_y-\psi_{1y})}{\tan(\psi_x-\psi_{1x})}\right] \end{gathered} \tag{29}$$

where

$$\begin{aligned} \tan\psi_x &= \tan\theta\cos\varphi \\ \tan\psi_y &= \tan\theta\sin\varphi \end{aligned} \tag{30}$$

Due to the axial symmetry of the bremsstrahlung emission and angular electron distributions, the folding integral can be reduced to

$$\begin{gathered} \frac{\mathrm{d}^2\sigma_f(\theta)}{\mathrm{d}k\mathrm{d}\Omega} = \int_{-\pi}^{\pi} d\psi_{1x}\int_{-\pi}^{\pi} d\psi_{1y}\frac{\mathrm{d}^2\sigma\left[\arctan\sqrt{\tan^2(\psi_x-\psi_{1x})+\tan^2(\psi_y-\psi_{1y})}\right]}{\mathrm{d}k\mathrm{d}\Omega}\times \\ F\left(\arctan\sqrt{\tan^2\psi_{1x}+\tan^2\psi_{1y}}\right) + P(\theta=0,d)\frac{\mathrm{d}^2\sigma(\theta)}{\mathrm{d}k\mathrm{d}\Omega} \end{gathered} \tag{31}$$

where we chosed that $\psi_x = \psi_y = \arctan(\tan\theta/\sqrt{2})$ in order to obtain a symmetric double folding integral, which is more suitable for a numerical treatment. Here, $P(\theta=0,d)$ denotes the probability that the electron is not deviated at the depth d in the target (given by Rel. 2). $P(\theta=0,d)$ is different from zero only in a thin slice at the entrance side of the target.

Electron slowing down

The slowing down of the electron is produced mainly by two effects: the inelastic collision and the bremsstrahlung production.

The mean energy loss due to inelastic collisions is given by the following numerical formulas appropriate for low and high incident energies[4]. The Bohr expression for the mean energy loss reads

$$-\frac{\mathrm{d}\bar{E}_c}{\mathrm{d}x} = 0.306\rho\left(\frac{Z}{A}\right)\beta^{-2}\ln\left(1.16\frac{E_k}{I}\right) \tag{32}$$

for $\beta < 0.5$ and the available Bethe –Bloch expression in the relativistic region is

$$\begin{gathered} -\frac{\mathrm{d}\bar{E}_c}{\mathrm{d}x} = 0.153\rho\frac{Z}{A}\beta^{-2}\left[\ln\frac{E_k(E_k+mc^2)^2\beta^2}{2I^2mc^2} + \left(1-\beta^2\right) - \right. \\ \left. 2\sqrt{1-\beta^2} - 1 + \beta^2\frac{1}{8}\left(1-\sqrt{1-\beta^2}\right)^2 - \delta\right] \end{gathered} \tag{33}$$

for $\beta \geq 0.5$. The mean energy loss is given in MeV/cm, the density ρ is considered in g/cm^2, here E_k is the kinetic energy in MeV, mc^2=0.51 MeV, and I are the ionization potentials which are listed in the literature[9]. The parameter δ is known as a density effect. The semi-empirical form of δ originally proposed by Sternheimer[10] is still used:

$$\delta = \begin{cases} 0 \quad \text{for} \quad X < X_0 \\ 4.606X + C + a(X_1 - X)^m \quad \text{for} \quad X_0 < X < X_1 \\ 4.606X + C \quad \text{for} \quad X_1 < X \end{cases} \tag{34}$$

where

$$X = \log_{10}\left(\frac{\beta}{(1-\beta^2)^{\frac{1}{2}}}\right) \tag{35}$$

is a velocity dependent parameter,

$$C = -2\ln\left(\frac{I}{\hbar\omega_p}\right) \tag{36}$$

is material dependent parameter, with $\omega_p^2 = 4\pi Ne^2/m$ being the bulk plasma frequency. Numerically $\hbar\omega_p = 30.47\left(\frac{Z\rho}{A}\right)^{1/2}$ in eV. The density ρ is expressed in g/cm^3, m=3,

$$a = -(C + 4.606X_0)/(X_1 - X_0) \tag{37}$$

$$X_0 = \begin{cases} 0.2 \text{ for } I < 100 \text{ eV and } |C| < 3.681 \\ 0.326|C| - 1 \text{ for } I < 100 \text{ eV and } |C| \geq 3.681 \\ 0.2 \text{ for } I \geq 100 \text{ eV and } |C| < 5.215 \\ 0.326|C| - 1.5 \text{ for } I \geq 100 \text{ eV and } |C| \geq 5.215 \end{cases} \tag{38}$$

$$X_1 = \begin{cases} 2 \text{ for } I < 100 \text{ eV and } |C| < 3.681 \\ 2 \text{ for } I < 100 \text{ eV and } |C| \geq 3.681 \\ 3 \text{ for } I \geq 100 \text{ eV and } |C| < 5.215 \\ 3 \text{ for } I \geq 100 \text{ eV and } |C| \geq 5.215 \end{cases} \tag{39}$$

The bremsstrahlung differential cross-section in photon energy formulas are obtained by using the prescriptions given by Koch and Motz[7]. The same forms were used in the electron slowing down evaluations of Pages and al.[11]:

$$\frac{\mathrm{d}\sigma}{\mathrm{d}k} = \begin{cases} f_E \frac{\mathrm{d}\sigma^{\mathrm{3BNa}}}{\mathrm{d}k} \text{ for } 0.01 \text{ MeV} < E_e < 0.1 \text{ MeV and } k \geq 0.01T_0 \\ \mathcal{A} f_E \frac{\mathrm{d}\sigma^{\mathrm{3BN}}}{\mathrm{d}k} \text{ for } 0.1 \text{ MeV} \leq E_e < 2 \text{ MeV and } k \geq 0.01T_0 \\ \mathcal{A}\frac{\mathrm{d}\sigma^{\mathrm{3BN}}}{\mathrm{d}k} \text{ for } 2 \text{ MeV} \leq E_e < 15 \text{ MeV and } \gamma \geq 15 \\ \mathcal{A}\frac{\mathrm{d}\sigma^{\mathrm{3BSd}}}{\mathrm{d}k} \text{ for } 2 \text{ MeV} \leq E_e < 15 \text{ MeV and } 2 < \gamma < 15 \\ \mathcal{A}\frac{\mathrm{d}\sigma^{\mathrm{3BSc}}}{\mathrm{d}k} \text{ for } 2 \text{ MeV} \leq E_e < 15 \text{ MeV and } 2 \leq \gamma \\ \frac{\mathrm{d}\sigma^{\mathrm{3BN}}}{\mathrm{d}k} \text{ for } 15 \text{ MeV} \leq E_e < 50 \text{ MeV and } \gamma \geq 15 \\ \mathcal{A}\frac{\mathrm{d}\sigma^{\mathrm{3BSd}}}{\mathrm{d}k} \text{ for } 15 \text{ MeV} \leq E_e < 50 \text{ MeV and } 2 < \gamma < 15 \\ \mathcal{A}\frac{\mathrm{d}\sigma^{\mathrm{3BSc}}}{\mathrm{d}k} \text{ for } 15 \text{ MeV} \leq E_e < 50 \text{ MeV and } \gamma \leq 2 \\ \frac{\mathrm{d}\sigma^{\mathrm{3BN}}}{\mathrm{d}k} \text{ for } 50 \text{ MeV} \leq E_e < 500\text{MeV and } \gamma \geq 15 \\ \frac{\mathrm{d}\sigma^{\mathrm{3CSa}}}{\mathrm{d}k} \text{ for } 50 \text{ MeV} \leq E_e < 500\text{MeV and } 2 < \gamma < 15 \\ \frac{\mathrm{d}\sigma^{\mathrm{3CSb}}}{\mathrm{d}k} \text{ for } 50 \text{ MeV} \leq E_e < 500\text{MeV and } \gamma \leq 2 \end{cases} \tag{40}$$

where

$$\frac{\mathrm{d}\sigma^{\mathrm{3BNa}}}{\mathrm{d}k} = \frac{Z^2 r_0^2}{137}\frac{16}{3}\frac{1}{p^2}\ln\left(\frac{p+p'}{p-p'}\right)\frac{1}{k} \tag{41}$$

$$p = \frac{\beta_0}{(1-\beta_0^2)^{1/2}} \tag{42}$$

$$\frac{\mathrm{d}\sigma^{\mathrm{3BN}}}{\mathrm{d}k} = \frac{Z^2 r_0^2}{137}\frac{p'}{p}\left[\frac{4}{3} - 2EE'\left(\frac{p'^2+p^2}{p^2p'2}\right) + \frac{\mathcal{E}E'}{p^3} + \frac{\mathcal{E}'E}{p'^3} + \frac{\mathcal{E}\mathcal{E}'}{pp'} + \mathcal{L}\mathcal{U}\right]\frac{1}{k} \tag{43}$$

$$\mathcal{E} = \ln\frac{E+p}{E-p} \tag{44}$$

$$\mathcal{E}' = \ln\frac{E'+p'}{E'-p'} \tag{45}$$

$$\mathcal{L} = 2\ln\left(\frac{EE'+pp'-1}{k}\right) \tag{46}$$

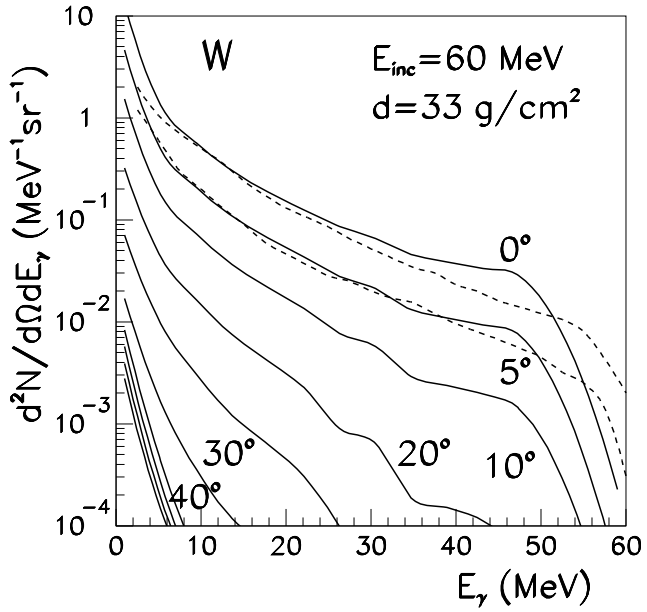

Figure 1: Angular and energy distributions of the bremsstrahlung emission per 60 MeV incident electron. The cylindrical converter is made from W, the thickness is 33 g/cm^2. The diameter is equal to the thickness. The full lines correspond to the present calculations. Some emission angles are marked on the plot. The results corresponding to 50° up 80°, in steps of 10°, are also displayed but the yields are lower. The dotted lines are extracted from the work of Berger and Seltzer[8] for (0–0.5)° and (0–5)°.

$$\mathcal{U} = \frac{8EE'}{3pp'} + k^2\frac{E^2E'^2 + p^2p'^2}{p^3p'^3} + \frac{k}{2pp'}\left[\left(\frac{EE'+p^2}{p^3}\right)\mathcal{E} - \left(\frac{EE'+p'^2}{p'^3}\right)\mathcal{E} + \frac{2kEE'}{p'^2p^2}\right] \tag{47}$$

$$\frac{\mathrm{d}\sigma^{\mathrm{3BSd}}}{\mathrm{d}k} = \frac{4Z^2r_0^2}{137}\left[1 + \left(\frac{E'}{E}\right)^2 - \frac{2}{3}\frac{E'}{E}\right]\left[\ln\frac{2EE'}{k} - \frac{1}{2} - c(\gamma)\right]\frac{1}{k} \tag{48}$$

$$c(\gamma) = 0.102\exp(-0.151\gamma) + 0.47\exp(-19.8\gamma) \tag{49}$$

$$\frac{\mathrm{d}\sigma^{\mathrm{3BSc}}}{\mathrm{d}k} = \frac{4Z^2r_0^2}{137}\left\{\left[1 + \left(\frac{E'}{E}\right)^2\right]\left[\frac{\phi(\gamma)}{4} - \frac{\ln Z}{3}\right] - \frac{2E'}{3E}\left[\frac{\phi_2(\gamma)}{4} - \frac{\ln Z}{3}\right]\right\}\frac{1}{k} \tag{50}$$

$$\begin{aligned}\phi_1(\gamma) &= \phi_2(\gamma) + 0.5\exp(-2.31\gamma) + 0.12\exp(-19.8\gamma)\\ \phi_2(\gamma) &= 20.14\exp(-0.151\gamma)\end{aligned} \tag{51}$$

$$\frac{\mathrm{d}\sigma^{\mathrm{3CSa}}}{\mathrm{d}k} = \frac{4Z^2r_0^2}{137}\left\{\left[1 + \left(\frac{E'}{E}\right)^2 - \frac{2E'}{3E}\right]\left[\ln\left(\frac{183}{Z^{1/3}}\right) - f(Z)\right] + \frac{E'}{9E}\right\}\frac{1}{k} \tag{52}$$

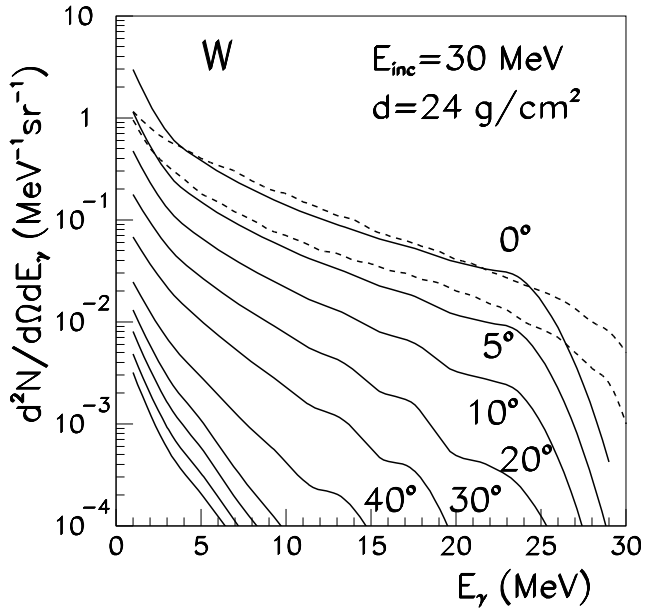

Figure 2: Angular and energy distributions of the bremsstrahlung emission per 30 MeV incident electron. The cylindrical converter is made from W, the thickness is 24 g/cm^2. The diameter is equal to the thickness. The full lines correspond to the present calculations. Some emission angles are marked on the plot. The results corresponding to 50° up 80°, in steps of 10° are also displayed but the yields are lower. The dotted lines are extracted from the work of Berger and Seltzer[8] for (0–0.5)° and (0–5)°.

$$f(Z) = \left[\frac{1}{1+(Z/137)^2} + 0.20206\right]\left(\frac{Z}{137}\right)^2 \tag{53}$$

$$\frac{\mathrm{d}\sigma^{3\mathrm{CSc}}}{\mathrm{d}k} = \frac{4Z^2 r_0^2}{137}\left\{\left[1+\left(\frac{E'}{E}\right)^2\right]\left[\frac{\phi_1(\gamma)}{4} - \frac{\ln Z}{3} - f(Z)\right] - \frac{2E'}{3E}\left[\frac{\phi_2(\gamma)}{4} - \frac{\ln Z}{3} - f(Z)\right]\right\} \tag{54}$$

The mean energy loss due to the radiative process is

$$\frac{\mathrm{d}\bar{E}_b}{\mathrm{d}x} = \frac{6.0249\times 10^{23} mc^2}{A}\int_0^{E_k} k\frac{\mathrm{d}\sigma}{\mathrm{d}k}\mathrm{d}k \tag{55}$$

so that the total energy loss is given by the relation

$$\frac{\mathrm{d}\bar{E}}{\mathrm{d}x} = \frac{\mathrm{d}\bar{E}_c}{\mathrm{d}x} + \frac{\mathrm{d}\bar{E}_b}{\mathrm{d}x} \tag{56}$$

Our numerical results agree within few percents with the previous publised values[11].

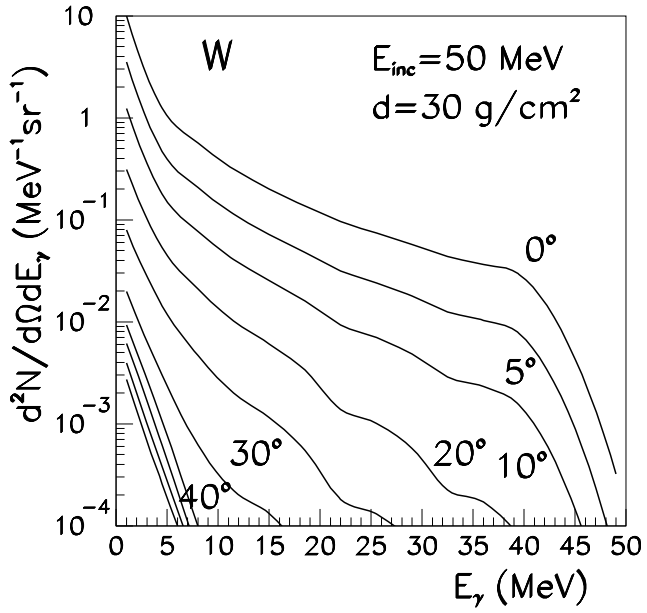

Figure 3: Angular and energy distributions of the bremsstrahlung emission per 50 MeV incident electron. The cylindrical converter is made from W, the thickness is 30 g/cm^2. The diameter is equal to the thickness. The full lines correspond to the present calculations. Some emission angles are marked on the plot. The results corresponding to 50° up 80°, in steps of 10° are also displayed but the yields are lower.

Other effects

As mentioned by Knop and Paul[4], for thick foils theoretical calculations are very difficult and only for complete diffusion it is possible to give an analytical expression for the angular distribution

$$F(\theta) = \frac{3}{4\pi}(0.717 + \cos\theta)\cos^2\theta \tag{57}$$

In order to improve the results at the end of the range, the angular distribution is varied linearly from that obtained with the multiple scattering formula to that available for complete diffusion (when the average energy of the electron in the target is less than 1/4 of the initial electron beam).

The endpoint region (high frequence) of the bremsstrahlung spectrum is corrected using the Fano formula[7]

$$\frac{\mathrm{d}^2\sigma}{\mathrm{d}\Omega \mathrm{d}k} = \frac{2Z^3 r_0^2 \beta \sin^2\theta}{137^2 k^3 E^3} \frac{1 + \frac{1}{2}E(E-1)(E-2)(1-\beta\cos\theta)}{(1-\beta\cos\theta)^4} \tag{58}$$

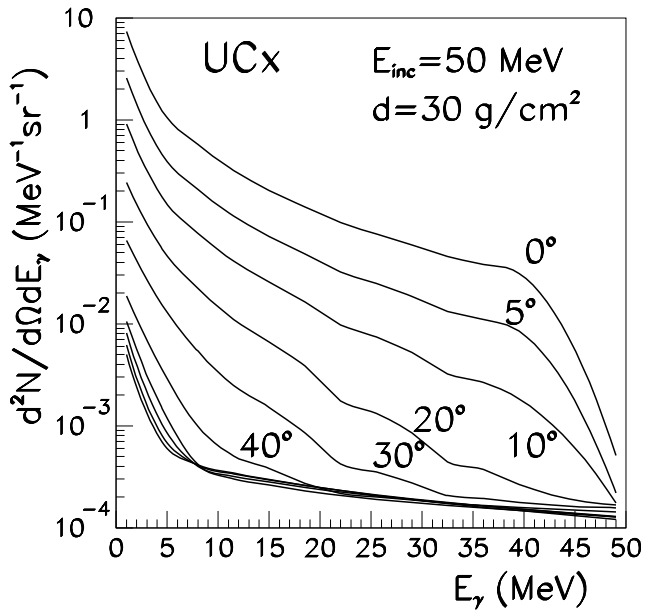

Figure 4: Angular and energy distributions of the bremsstrahlung emission per 50 MeV incident electron. The cylindrical converter is made from UCx, the thickness is 30 g/cm^2. The diameter is equal to the thickness. The full lines correspond to the present calculations. Some emission angles are marked on the plot. The results corresponding to 50° up 80°, in steps of 10° are also displayed but the yields are lower.

A linear interpolation is used in the way similar to that used by Berger and Seltzer[8] in the region $0.85T < k < T$, T being the kinetic energy of the electron. The different cross section formulas are smoothly joined during the passage of their appropriate limits of validity by mean of a linear interpolation. This procedure avoids abrupt variations of the cross section in the vicinity of the limits of validity.

The effect of mixtures can be included in computing the lateral and angular deflections by replacing NZ^2 by $\sum_i N_i Z_i^2$ summed on different atomic species[6], N_i being the number of atom of the specie i in the volume unity. To compute the slowing down and the bremsstrahlung cross section, the effective values of the target parameters can be deduced using the Bragg rule[12,13] which stipulates that the stopping of the individual elements are approximately additive. The same rule is valid for the gamma absorption coefficients[14].

RESULTS AND DISCUSSION

The primary purpose of our calculations was to obtain the bremsstrahlung spectra of interest for the design of a neutron rich nuclei source based on the gamma induced fission of ^{238}U. For that purpose, high gamma yields at energies around 10 MeV are necessary, focussed as best as

possible in the forward direction, in order to produce a large number of fission events in the fissionable target placed in the vicinity of the converter. A numerical tool was conceived to estimate quickly these spectras. So, our analysis is mainly dedicated to small angles, where we need a good precision of our simulations, or, at least, an information about the degree of accuracy of our evaluation. Having in mind that the bremsstrahlung spectrum emitted at 0° is harder and more intense that the spectra obtained in other directions, this evaluation will help to conceive the radiative shielding of the source in the critical conditions. In the following work, the bremsstrahlung emissions of cylindrical W and UCx targets are simulated for initial energies of the electrons included in the interval 30–60 MeV. The converter thicknesses are considered twice the range of the electron to allow comparisons with previous published results. In Fig. 1, the spectra $d^2N/\mathrm{d}\Omega\mathrm{d}E_\gamma$ of the bremsstrahlung emerging at various directions from a thick W target for an incident electron energy of 60 MeV are represented. Here N is the number of photons, E_γ is the gamma energy in MeV. At the small angles 0° and 5°, Monte-Carlo simulations[8] for W target of same thickness can be compared. As expected, the high energy bremsstrahlung yields are larger in the vicinity of a small region around the 0° emergence angle. As specified[8], the high energy bremsstrahlung can be emitted only by electrons that have lost little energy and, consequently, have not yet deflected much by multiple scattering. Generally, our forward direction values of the spectra agree with those of Berger and Seltzer[8] within 20%. However, larger deviations appear in the high energy region, where $E_\gamma > 0.9E_{inc}$, E_{inc} being the energy of the beam. These differences can be understood as follows: in the high energy region, we used different methods to correct the cross section. In this paper, the analytical Fano formula is kept while in the cited work[8], an interpolation with experimental data was done. In Fig. 2, the same quantities are plotted for an incident electron energy of 30 MeV. Similar trends as in Fig. 1 are displayed, but the yield at 10 MeV is lowered by a factor 3. From these examples, we illustrated the degree of accuracy of our simulations. Our interest is now focussed on initial energies of 50 MeV, because from considerations which are not of physical nature, it is expected that our future facility will deliver about 50 MeV electron beam. The results concerning the 50 MeV electron beam onto W are displayed in Fig. 3. It seems that this energy is in fact suitable for our purpose because the yields of the forward spectra are only 20–30% lower in the vicinity of $E_\gamma \approx$10 MeV than those obtained at 60 MeV incident energy. This decrease is not dramatic, and we avoid the production of intense gamma yields in the 50-60 MeV region. The next step is the study of the radiative bremsstrahlung emission from the UCx target, when the 50 MeV electron beam impinges directly on the target (without converter). The ratio between the number of C atoms versus that of U is 2.5 and the density of the mixture is 3.6 g/cm^3. Using the formulae presented in the previous section, the range of 50 MeV electrons in the mixture was calculated as about 14.5 g/cm^2, being not too different than that in the W converter. Accordingly, for a comparison purpose with the results corresponding to the W converter, the thickness was taken also 30 g/cm^2 (approximately twice the range). The spectra obtained for the UCx target are presented in Fig. 4. Practically, the forward direction spectra have the same shapes as those in the case of the W converter. Having in mind that focusing the electron beam directly on the fissionable target, the bremsstrahlung radiation emitted in all the directions enhances the fission events number, it can be expected that the neutron rich nuclei productivity of the source increases. By placing the intermediate converter, a large amount of gamma rays emitted at larger angles cannot reach the target. It can be also noted that the UCx spectra obtained at larger angles are greater than those obtained for the W converter. Finally, this study gives evidence for the advantages obtained by eliminating the intermediate converter and offers the possibility to estimate the required radiative shield of our combination. Furthermore, the numerical code developed will permit the evaluation the efficiency dependence for different quantities of the neutron rich ion source (such as the number of fission events) in order to optimize the yields.

ACKNOWLEDGEMENTS

This work was sponsored by the European Contracts SPIRAL II No. ERB 4062 PL 975009, No. FMGE CT 980100 and by the IDRANAP European Center of Excellence.

REFERENCES

1. F. Clapier, A.C. Mueller, C. Obert, O. Bajeat, M. Ducourtieux, A. Ferro, A. Horbowa, L. Kotfila, C. Lau, H. Lefort, S. Kandri–Rody, N. Pauwels, J.C. Poitier, J. Proust, J.C. Putaux, C.F. Liang, P. Paris, A.C.C. Vilari, R. Lichtenhaler, L. Maunoury and J. Lettry, *Exotic Beams Produced by Fast Neutrons*, Phys. Rev. ST Accel. Beams **1**, 013501(3) (1998).

2. S. Kandri–Rody, J. Obert, E. Cottereau, O. Bajeat, M. Ducourtieux, C. Lau, H. Lefort, J.C. Potier, J.C. Putaux, F. Clapier, J. Lettry, A.C. Mueller, N. Pauwels, J. Proust, C.F. Liang, P. Paris, H.L. Ravn, B. Roussiere, J. Sauvage, J.A. Scarpaci, F. Le Blanc, G. Galu, I. Lhenry, T. Von Egidy and R. Antoni, *Exotic Nuclei Produced by Fast Neutrons in a Liquid Uranium Target*, Nucl.Instr.Meth. B **160**, 1–6 (2000).

3. M. Mirea, O. Bajeat, F. Clapier, F. Ibrahim, A.C. Mueller, N. Pauwels and J. Proust, *Modeling a Neutron Rich Nuclei Source*, Eur. Phys. J. A **11**, 59–78 (2001).

4. G. Knop and W. Paul, *Interaction of Electrons and α–Paricles with Matter* in *Alpha-, Beta- and Gamma-Ray Spectroscopy*, edited by K. Siegbahn, North Holland Publ. Co. Amsterdam, chap. 1, p. 1, (1968).

5. W.A. McKinley Jr. and H. Feshbach, *The Coulomb Scattering of Relativistic Electrons by Nuclei*, Phys. Rev. **74**, 1759–1763 (1948).

6. W.T. Scott, *The Theory of Small Angle Multiple Scattering of Fast Charged Particles*, Rev. Mod. Phys. **35**, 231–313 (1963).

7. H.W. Koch and J.W. Motz, *Bremsstrahlung Cross–Section Formulas and Related Data*, Rev. Mod. Phys. **31**, 920–955 (1950).

8. M.J. Berger and S.M. Seltzer, *Bremsstrahlung and Photoneutron from Thick Tungsten and Tantalum Targets*, Phys. Rev. C **2**, 621–631 (1970).

9. S.P. Ahlen, *Theoretical and Experimental Aspects of the Energy loss of Reletivistic Heavily Ionizing Particles*, Rev. Mod. Phys. **52**, 121–173 (1980).

10. R.M. Sternheimer, *The density Effect for the Ionization Loss in Various Materials*, Phys. Rev. **88**, 851–859 (1952).

11. L. Pages, E. Bertel, H. Joffre and L. Sklavenitis, *Energy Loss, Range, and Bremsstrahlung Yield for 10 keV to 100 MeV Electrons in Various Elements and Chemical Compounds*, At. Data **4**, 1-127 (1972).

12. W.R. Leo, *Passage of Radiation through Matter* in *Techniques for Nuclear and Particle Physics Experiments*, Springer Verlag Berlin, Heildelberg, New York, chap. 2, p. 17, (1987).

13. R.M. Sternheimer, *Interaction of Radiation with Matter* in *Methods of Experimental Physics*, Ed. by L.C.L. Yuan and C.S. Wu, Academic Press, New York, Vol. 5, Part A, chap. 1.1, p. 1., (1961).

14. C.M. Davisson, *Gamma–Ray Attenuation Coefficients* in *Alpha–, Beta– and Gamma–Ray Spectroscopy*, Ed. by K. Sieghbahn, North Holland Publ. Co. Amsterdam, appendix 1, p. 827, (1968).